Fuzzy Logic Speed Control for Three-Phase Induction Motor Supplied by Photovoltaic System with a Robust MPPT

Ali M. Yousef*, Farag K. Abo-Elyousr**

*Electrical Eng. Dept., Faculty of Engineering, Assiut University, Assiut, Egypt, email:

**Electrical Eng. Dept., Faculty of Engineering, Assiut University, Assiut, Egypt

Drali_yousef@yahoo.com

Abstract:- This paper proposes a speed control method based on fuzzy logic and conventional PI controller for a three-phase induction motor fed by a photovoltaic generator. The speed for induction motor has been controlled using an inverter driven by space vector pulse width modulation (SVPWM) technique. The SVPWM inverter operates according to the voltage and frequency (V/F) control method. In this work, numerous practical aspects related to the induction motor speed changes operation have been considered. The photovoltaic generator and motor performance is investigated with the maximum power point tracking (MPPT) and without MPPT control. The results of the simulation conducted using the new proposed control method demonstrates the effectiveness of the proposed fuzzy controller compared with the conventional PI controller.

Keywords: Three–phase induction motor, V/F control, MPPT, Fuzzy Logic Control, PI control

Nomenclature

I_o : The reverse saturation current
I_{ph} : The light generation current
I : The photoelectric output current
I_{sc} : The short circuit current
A : The ideality factor
V : The photoelectric voltage
R_s : The module series resistance
n_s : The number of series connected solar cells
k : The Boltzmann's constant
q : The magnitude of the electron charge
T : The absolute temperature
G : The isolation value
I_{PV} : the Photovoltaic array current
t : time
P : number of poles
J : machine moment of inertia
ω_m , ω_r : rotor mechanical and electrical speeds respectively
V_n : nominal motor voltage,
f_n : Motor rated frequency

1. Introduction

Induction motors are widely used in industrial applications and in automotive propulsion industry. Modern adjustable speed drives of three-phase induction machines make induction motors to be recognized as strong candidates for propulsion in electric hybrid and pure electric road vehicles. They require AC supply to produce rotating field. The AC current can be produced using and inverter [1]. Due to frequent starting and load changing conditions, robust speed control becomes very important.

Inherently, induction motors do not provide wide speed variation. In addition to that, induction motors have nonlinear dynamical characteristics [2]. Induction motors fed by PV energy are reliable and have low maintenance. For such applications, DC-DC converter and DC-AC inverter are used in order to achieve the motor power conversion [3]. Therefore, adjustable speed drives have a significant impact upon the induction motor performance in electromechanical systems. Because of its simplicity, scalar control is still one of the widely induction motor speed control [4].

Normally, the scalar control techniques include varying the voltage or frequency magnitudes or both. The constant voltage per frequency (V/F) control generates three-phase reference voltages proportional to the command or required speed. The magnitude of the stator voltages is adjusted in proportion to the frequency to maintain the motor flux constant. Voltage source inverters (VSI) with the space vector pulse width modulation (SVPWM) inverters are used to meet the above requirements for controlling the speed of an induction motor [4]. The reference voltage vector (V*) representing the three-phase voltage is generated using the SVPWM by switching between two adjacent active vectors and the zero vector as shown in Fig. 1 [5].

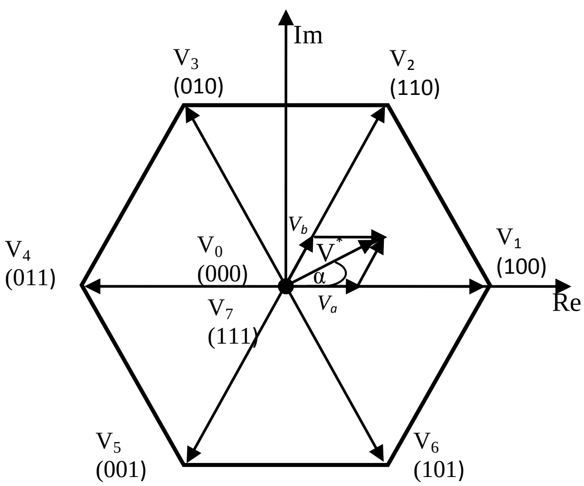

Fig. 1: Space vector modulation.

There are many methods for controlling motors speed such as the classic PID controller, modern controller (adaptive and improving), and intelligent controllers (fuzzy and neural) [3, 6, 7]. Classic PID controllers are offline controllers. These controllers are not effective if plant involved is higher order, nonlinear systems, complex, vague systems without accurate mathematical models, and systems with uncertainties. Therefore, speed or machines performance at transient variable speed tracking may be problematic [8, 9].

Fuzzy logic controller is online control. Recently, the fuzzy logic has been utilized for various control applications including motor speed control techniques [10, 11]. The fuzzy logic has made the control of complex nonlinear dynamic systems as simple as possible [10]. The full information measurements problem is then solved using nonlinear design tools for a suboptimal solution. This design paradigm has been applied to worst-case parameter identification problems [12], which has led to new classes of parameterized identifiers for linear and nonlinear systems. The technique has also been applied to adaptive control problems, and offered a promising tool to system subjected to uncertainties. [13-17].

The key contribution of the fuzzy logic control system is the fuzzy logic rules. The fuzzy logic rules are designed and optimized by the designer. In addition to that, the way to manipulate the fuzzy logic control input and output is an essential procedure. In this research, the classical PI and Intelligent fuzzy logic controller are designed and applied to speed control of a three-phase induction motor fed directly by PV generator through V/F VSI inverter. The impact of PV generator upon the induction motor behavior is investigated in this paper. Two cases are considered and compared to track a reference speed of an induction motor. The first case is operating the induction motor at adjustable speeds to extract the maximum available power from the PV generator. In some industrial PV applications, minimizing the cost of an operating system is required. The Maximum power point tracking (MPPT) algorithm is eliminated in such applications [3]. Therefore, the dynamics of operating the motor to track a reference speed without MPPT are investigated in this paper. The induction motor speed is controlled by an inverter driven by space vector pulse width modulation (SVPWM) technique. The operation of the SVPWM inverter is based on the voltage over frequency V/F control Method. Two VSI inverter topologies are investigated. Time-Based simulation results are carried out to verify the effectiveness of the proposed fuzzy logic control scheme under the transient and steady state operating conditions.

2. Power System Model

The power system model under study consists of photovoltaic (PV) system connected to an induction under maximum power point tracking as shown in Fig. 1. The system consists of PV system, MPPT algorithm, speed controller, and V/F VSI inverter.

Normally, the MPPT is achieved using a DC-DC converter.

2.1. Solar Cell Model

Solar cell mathematical modeling is an important step in the analysis and design of PV control systems to obtain the MPPT. The PV mathematical model can be obtained by following [15].

$$I_c = I_{ph} - I_o \left\{ e^{\left[\frac{q}{AkT}(V_c + I_c R_s) \right]} - 1 \right\} \quad (1)$$

$$V_c = \frac{AkT}{q} \ln\left(\frac{I_{ph} + I_o - I_c}{I_o} \right) - I_c R_s \quad (2)$$

$$I = I_{ph} - I_o \left\{ e^{\left[\frac{q}{n_s AkT}(V + n_s I R_s) \right]} - 1 \right\} \quad (3)$$

$$V = \frac{n_s AkT}{q} \ln\left(\frac{I_{ph} + I_o - I}{I_o} \right) - n_s I R_s \quad (4)$$

Where;

$$I_{ph} = \frac{G}{1000}[I_{sc} + k_i (T - T_r)]$$

$$I_o = I_{or} \left(\frac{T}{T_r} \right)^3 e^{\left[\frac{qE_g}{AK}\left(\frac{1}{T_r} - \frac{1}{T} \right) \right]}$$

The module output power can be determined simply from

$$P = VI \quad (5)$$

Figure 2 depicts the PV characteristics with with varying the insolation. Also, the I-V relation of the PV cell with the variation of insolation is showing in Fig. 3.

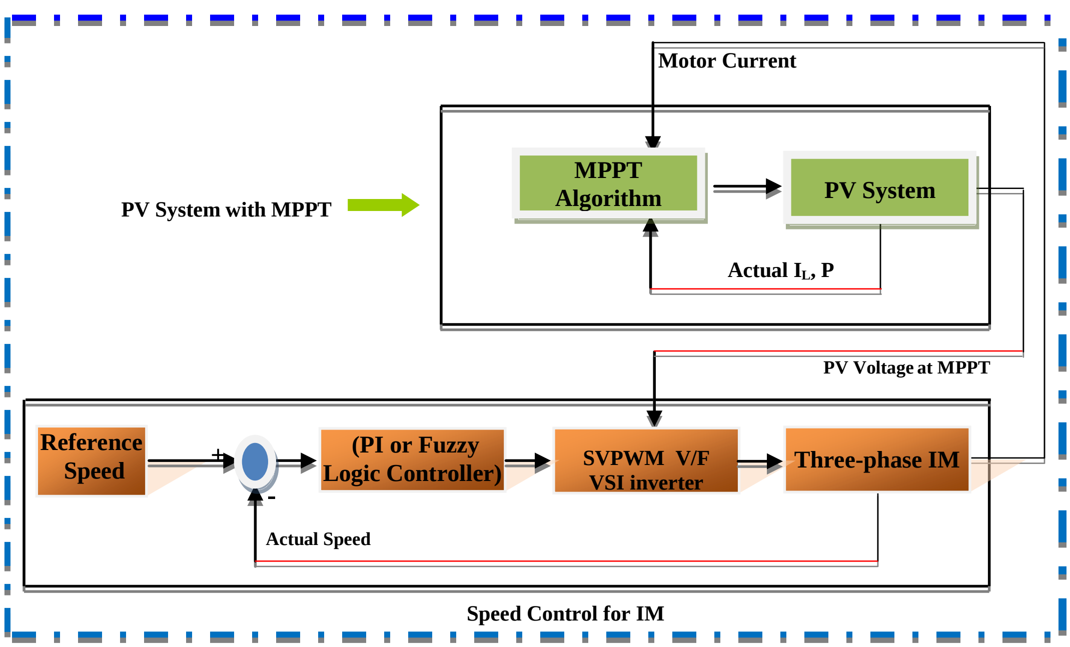

Fig. 1: Overall block diagram of IM motor control system supplied by PV system with MPPT.

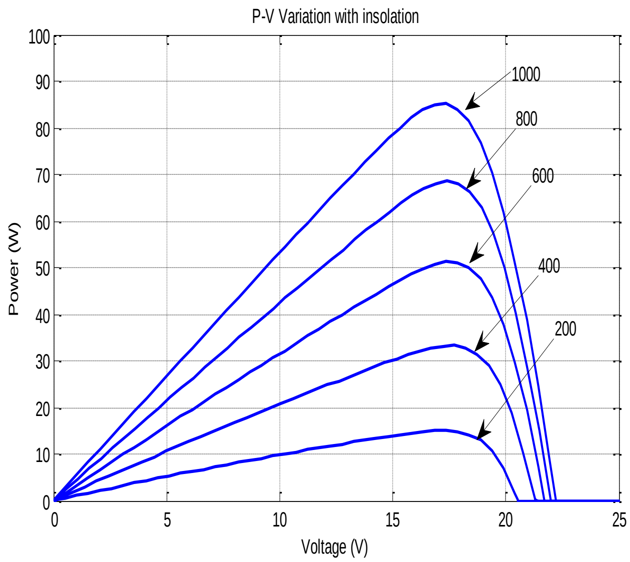

Fig. 2: P-V with variation of insolation

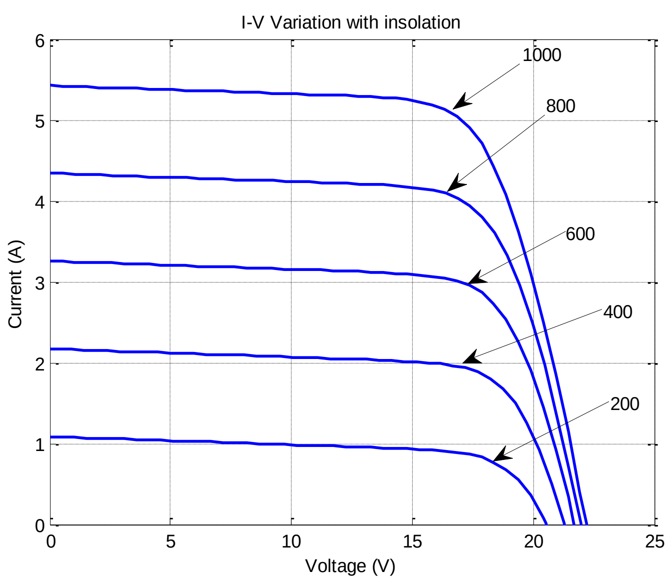

Fig. 3: I-V with variation of insolation

2.2. Maximum Power Point Tracking

The main purpose of the MPPT is to move the PV array operating voltage and current close to the maximum power value under variable changing atmospheric conditions and load. The method used to achieve the MPPT is based on the perturbation and observation technique [18-20]. Figure 4 shows the block diagram implementation of the MPPT algorithm.

The maximum power point tracker operates periodically by incrementing or decrementing the solar array voltage. Consequently, the perturbation leads increase or decrease in the PV array power. The algorithm starts by reading the power (P) values of the PV array. The PV array power is compared with the old values. The parameters Inc is given in (6).

$$Inc = \begin{cases} +1 & if \;\; P > P_{old} \\ -1 & if \;\; P < P_{old} \end{cases} \tag{6}$$

In Fig. 4, the parameter *ΔI* should be designed by the user. The controller may oscillate around the MPP forward and backward and may lack the speed for tracking in fast atmospheric changes. However, for small values of *ΔI*, the PV MPPT tracking can work well. Finally, the current is updated according to (7) after considering the PV current constraints.

$$\begin{aligned} I_{ref}(k+1) &= I_{ref}(k) + Inc \times \Delta I \\ I_{PV} &= I_{ref} \end{aligned} \tag{7}$$

2.3. Induction Motor Model

A generalized model of the induction motor (IM) can be expressed in the abc reference frame or in the dq stationery or rotating reference frame [14, 22]. In this research, an asynchronous model available in Matlab/Simulink will be used. The parameters data of the motor are given in Appendix A.

Driving the mathematical equations of an induction motor in dq stationery reference frame is given as shown in Fig. 5 [14]. The corresponding stationery frame equations are given in terms of the flux linkage expressions as follows:

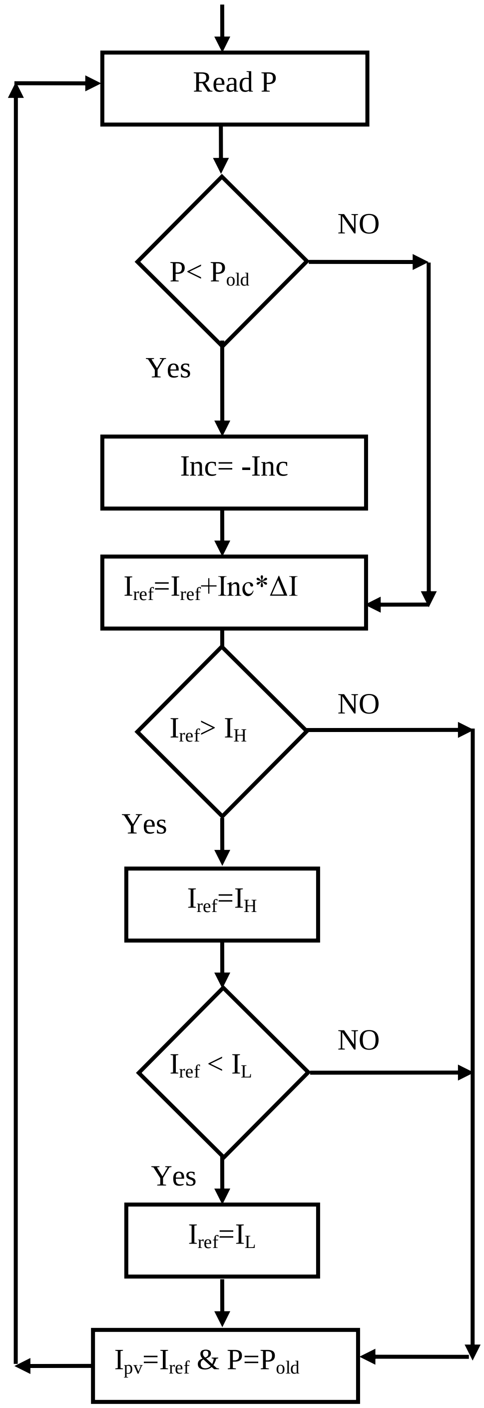

Fig. 4: MPPT Algorithm block flow chart

$$v_{qs} = R_s i_{qs} + \frac{d\psi_{qs}}{dt} \quad (8)$$

$$v_{ds} = R_s i_{ds} + \frac{d\psi_{ds}}{dt} \quad (9)$$

$$0 = R_r i_{qr} + \frac{d\psi_{qr}}{dt} - \omega_r \psi_{dr} \quad (10)$$

$$0 = R_r i_{dr} + \frac{d\psi_{dr}}{dt} + \omega_r \psi_{qr} \quad (11)$$

The flux linkage expressions are given as below.

$$\psi_{qs} = L_{ls} i_{qs} + L_m (i_{qs} + i_{qr}) \quad (12)$$

$$\psi_{qr} = L_{lr} i_{qr} + L_m (i_{qs} + i_{qr}) \quad (13)$$

$$\psi_{ds} = L_{ls} i_{ds} + L_m (i_{ds} + i_{dr}) \quad (14)$$

$$\psi_{dr} = L_{lr} i_{dr} + L_m (i_{ds} + i_{dr}) \quad (15)$$

The electromagnetic torque and the rotor mechanical and electrical speeds are given in (16), (17), (18) respectively.

$$T_e = 1.5 \left(\frac{P}{2} \right) \left(\psi_{ds} i_{qs} - \psi_{qs} i_{ds} \right) \quad (16)$$

$$\frac{d\omega_m}{dt} = \frac{(T_e - T_m)}{J} \quad (17)$$

$$\omega_r = \omega_m \times \frac{P}{2} \quad (18)$$

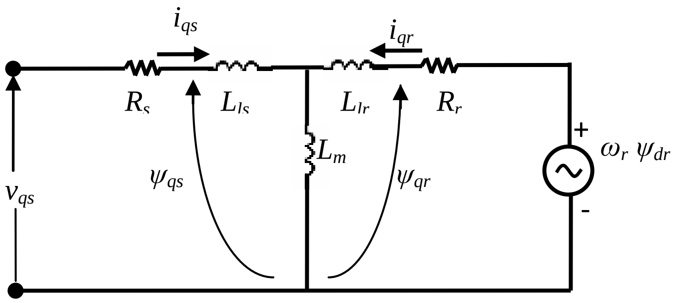

(a) q-axis equivalent circuit

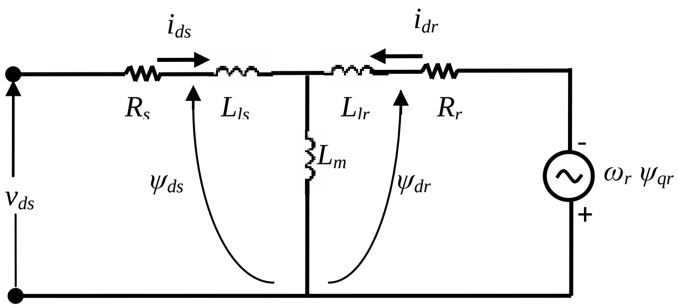

(a) d-axis equivalent circuit

Fig. 5: induction motor stationery d-q equivalent circuit model

2.4. V/F Theoretical Background

The output of the fuzzy logic or conventional PI controllers represents a frequency signal as shown in Fig. 6. This signal is converted into three sinusoidal signals shifted by 120 electrical degrees according to the next equations.

$$f_1(t) = f_e \frac{V_n}{f_n} \sin(2\pi f_e t) \tag{19}$$

$$f_2(t) = f_e \frac{V_n}{f_n} \sin(2\pi f_e t - \frac{2\pi}{3}) \tag{20}$$

$$f_1(t) = f_e \frac{V_n}{f_n} \sin(2\pi f_e t - \frac{4\pi}{3}) \tag{21}$$

$$f_e(t) = \frac{P}{2} \frac{\omega_e}{2\pi} \tag{22}$$

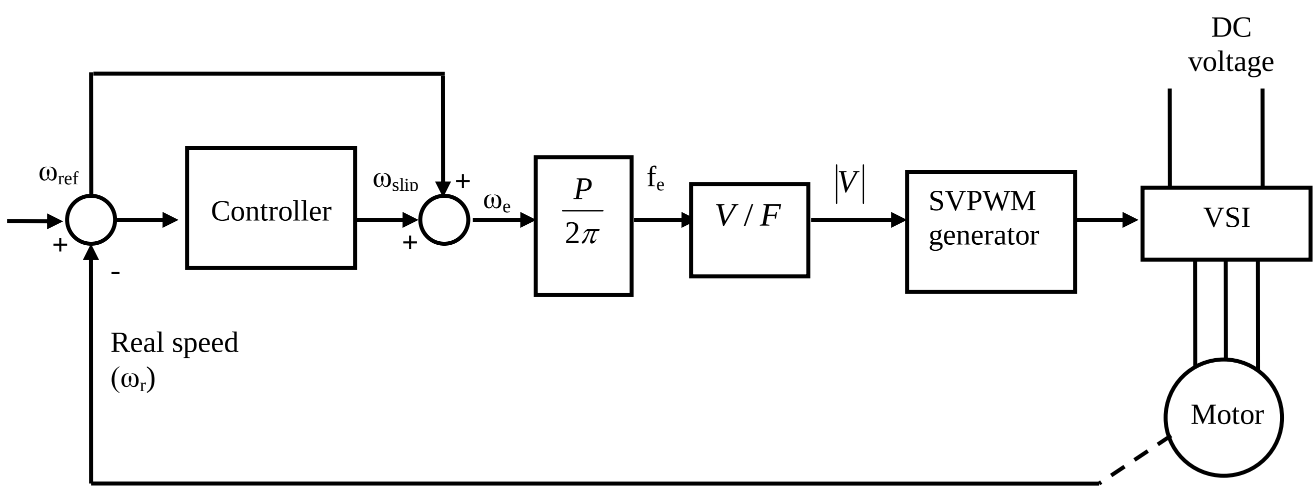

Fig. 6: V /F drive implementation

The amplitude and frequency of equations (19) to (21) varies according to the operating speed. Figure 7 shows how the V/F varies with the time. The reference speed is shown in Fig. 8.

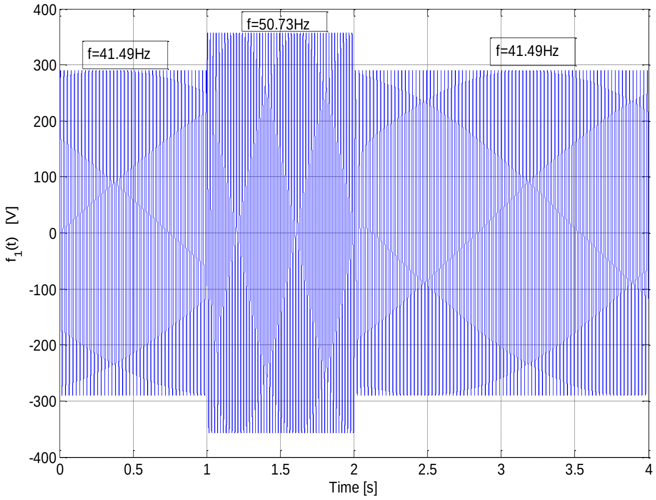

Fig.7: V /F variation with time

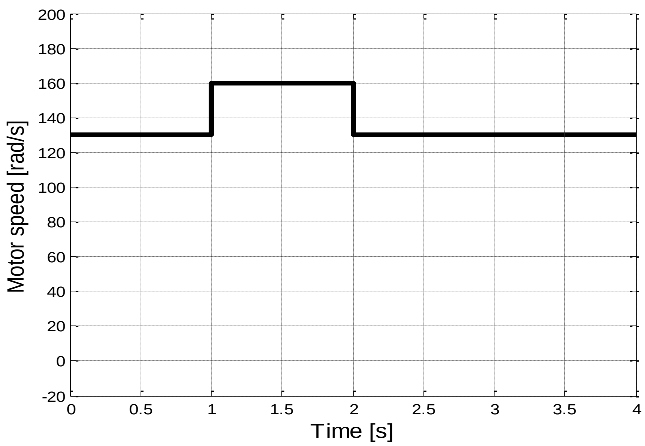

Fig. 8: Reference speed variation profile

2.5. SVPWM Inverter

Two VSI inverter topologies impact upon the induction motor speed performance are investigated in this section. The first topology is the universal three-leg inverter as shown in Fig. 9. Carrier based SVPWM is used to generate the switching patterns of the conventional bridge switches. Three sinusoidal input signals are used as in Fig. 10. The addition of the maximum and minimum signal of the three input signals are rescaled and added together to the input signal individually. This yields the duty ratio operation profile as shown in Fig. 11. By comparing the duty ratio profile with a high order frequency triangular carrier, switching pulses patterns can be generated [23].

The second topology is the three-level bridge inverter as depicted in Fig. 12. The line to line voltage of the both topologies is shown in Figs. 13 and 14 respectively. The three-level bridge inverter show better performance than the universal three-leg bridge. The line to line voltage is closer to the sinusoidal waveform in case of the two-level bridge. The switching patterns of the two-level bridge are given in [24].

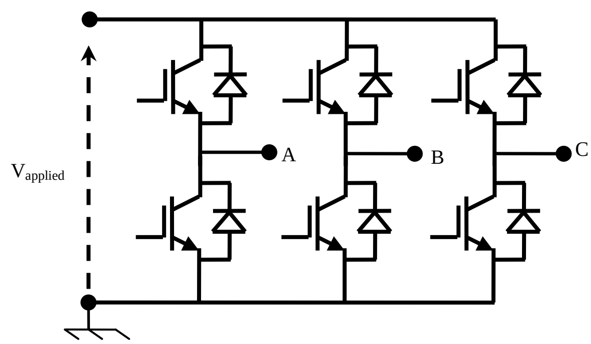

Fig. 9: Universal 3-leg inverter

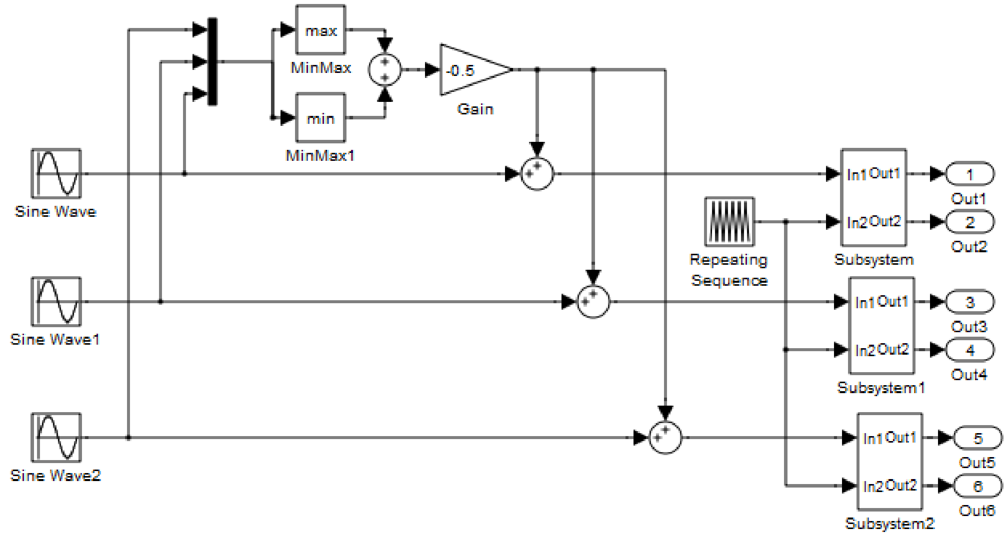

Fig. 10: Simulink model of carrier based SVPWM

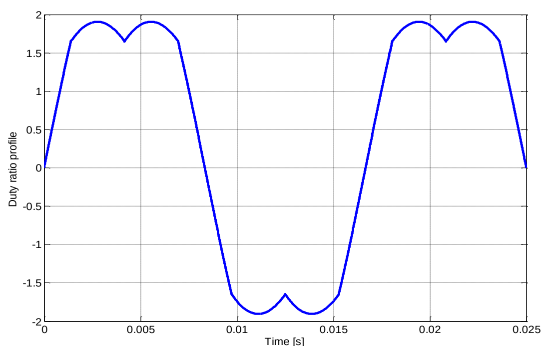

Fig. 11: Duty ratio profile of the first leg of the universal bridge

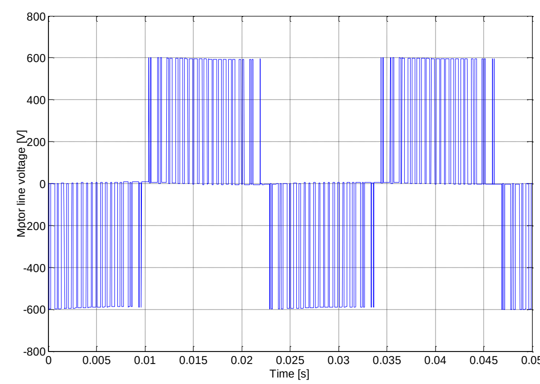

Fig. 13: Line to line voltage with 3-leg universal bridge

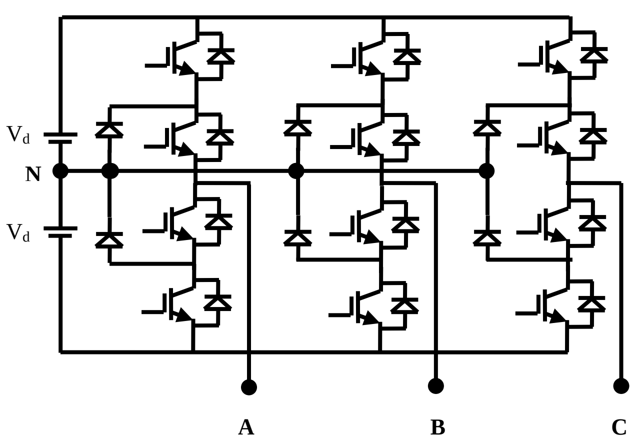

Fig. 12: Three-level bridge inverter

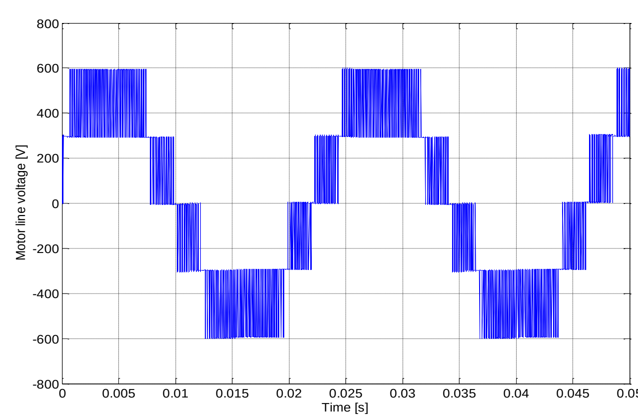

Fig. 14: Line to line voltage with 3-level bridge inverter

3. Proposed Controller

Two types of control are designed: fuzzy logic and conventional PI control.

3.1. Conventional PI control

The transfer function of the conventional PI controller is:

$$G_s(s) = K_p + K_I / s \quad (23)$$

If *e(t)* is the input to the **PID** controller, the output CPI from the controller is given by:

$$CPID = K_p e(t) + K_I \int e(t)dt \quad (24)$$

Thus at any instant of time the controller output is composed of two terms. One term is due to the accumulated area of error versus time, and the other is due to the present extent of the error [15].

The Proportion**:** can increase the response output controller and control accuracy of the system.

The Integration**:** is used to eliminate the steady-state error of the system (one reason is that the integral action gives the system the capability to adjust itself to new load conditions that require changes in the zero error control output (resetting action).

Figure 15 shows the speed response using the conventional PI controller. In addition to the superiority of voltage profile of the two-level bridge compared to the universal bridge, the speed response is a little better at step changes transient points. Therefore, the two-level bridge will be used in the next simulation results.

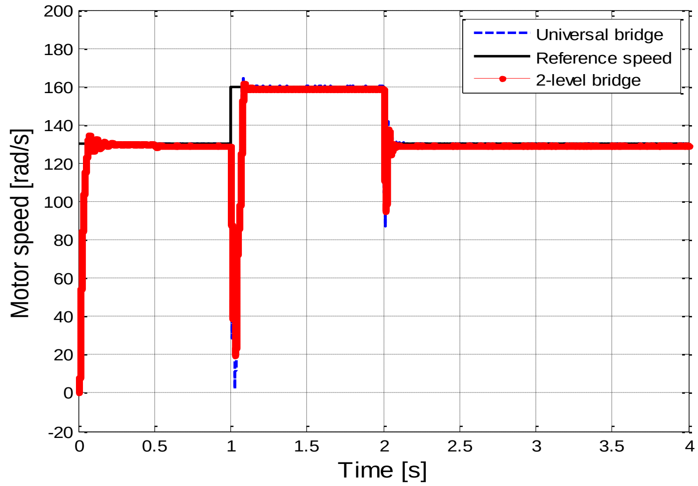

Fig. 15: IM speed variation response with conventional PI

3.2. Fuzzy logic Control

Fuzzy logic and conventional PI controllers are designed and applied to achieve reasonable rise time, settling time, overshoot and steady state error. The proposed strategy minimizes the error of the reference motor speed. Fuzzy logic has an advantage over other control methods due to the fact that it is not sensitive to plant parameter variations. The fuzzy logic control approach consists of three stages, namely fuzzification, fuzzy control rules engine, and defuzzification.

To design the fuzzy logic load frequency control, the input signal is the frequency deviation at sampling time and its change. While, the output signal is the change of the control signal ΔU(k). When the value of the control signal time [k-1] (U(k-1) is added to the output signal of the fuzzy logic controller, the required control signal U(k) is obtained. Fig. 16 shows the three-stage of fuzzy logic controller. The fuzzy logic control system is described in Fig. 17. The fuzzy control rules are illustrated in Table 1. The membership function shapes of the error, derivative error, and the gains are chosen to be identical with triangular function of the fuzzy logic control. However, this horizontal axis range takes different values because of optimizing the controller. The membership function sets of FLC for the induction motor are shown in Fig. 18.

Table 1: fuzzy logic control rules (Δf).

Δf	$d\ \Delta f$						
	LN	MN	SN	Z	SP	MP	LP
LN	LP	LP	LP	MP	MP	SP	Z
MN	LP	MP	MP	MP	SP	Z	SN
SN	LP	MP	SP	SP	Z	SN	MN
Z	MP	MP	SP	Z	SN	MN	MN
SP	MP	SP	Z	SN	SN	MN	LN
MP	SP	Z	SN	MN	MN	MN	LN
LP	Z	SN	MN	MN	LN	LN	LN

Where;
LN: large negative membership function;
MN: medium negative;
SN: small negative;
Z: zero; SP: small positive;
MP: medium positive;
LP: large positive.

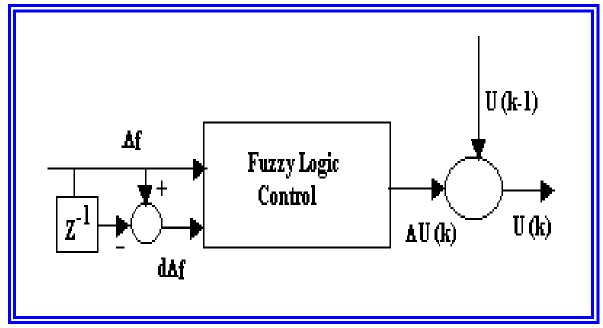

Fig. 17: Fuzzy logic control

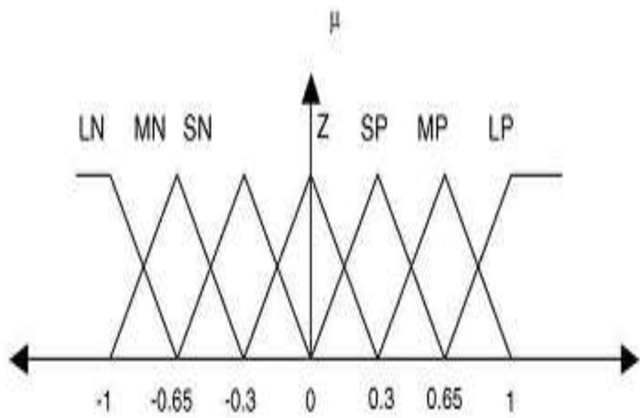

Fig. 18: The features of a membership function

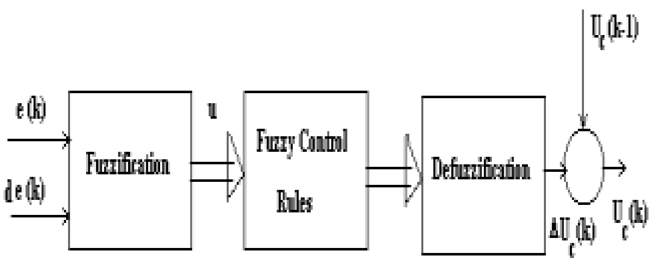

Fig. 16: Three-stage of fuzzy logic controller: u, membership degree

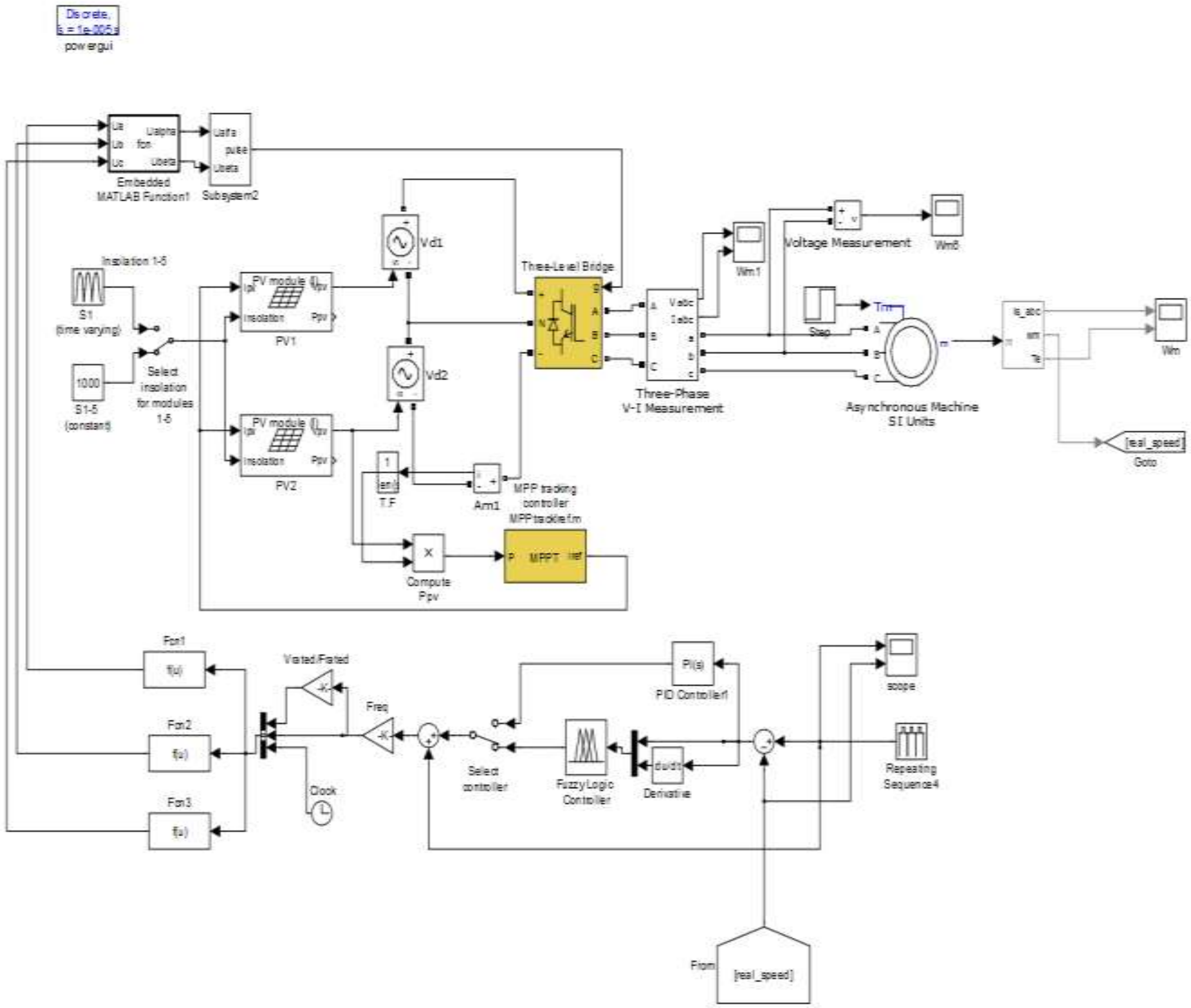

4. Simulation Results and Discussion

Figure 19 shows the Simulink model of PV-supplied induction motor with fuzzy and PI speed control. The induction machine parameters are given in Appendix A. The speed controller is applied by using the Conventional PI controller and the proposed fuzzy logic controller in two cases: one with using MPPT and another without MPPT.

4.1. Speed Control with MPPT

Figure 20 shows the motor current variation response in rms value with using the PI and fuzzy controllers with MPPT. The speed signal command is given in Fig. 8. The fuzzy logic controller shows lower current peaks at the transitorily change instants. Figure 21 depicts the motor speed variation response with PI and fuzzy controllers with MPPT. During the motor starting, it is noted that there is no speed overshoot related to the fuzzy controller speed response. The maximum undershoot values related to the fuzzy logic controller at 1s and 2s is small in comparison to the classic PI controller.

The voltage of PV cell variation response by using the PI and fuzzy controllers with MPPT is shown in Fig. 22. At the long term operating conditions, the PV output voltage shows higher values in case of the fuzzy logic controller. The better operating voltage behavior at the long term operating conditions results in better PV power profile with using the fuzzy logic controller as shown in Fig. 23. All last figures show the induction motor speed and current variation response are better with the proposed fuzzy logic controller than the conventional PI controller.

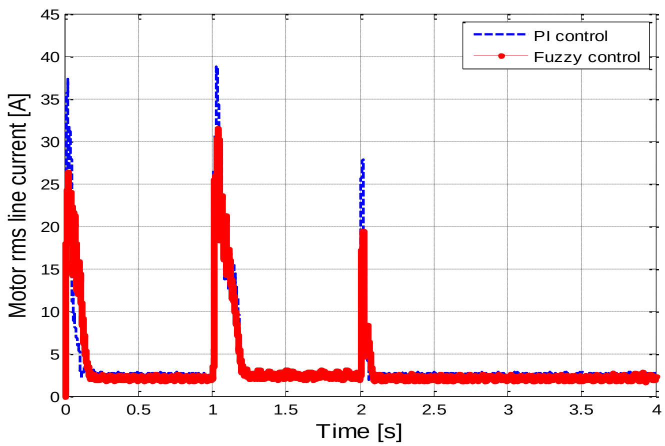

Fig. 20: The motor current variation response with PI and fuzzy controller with MPPT

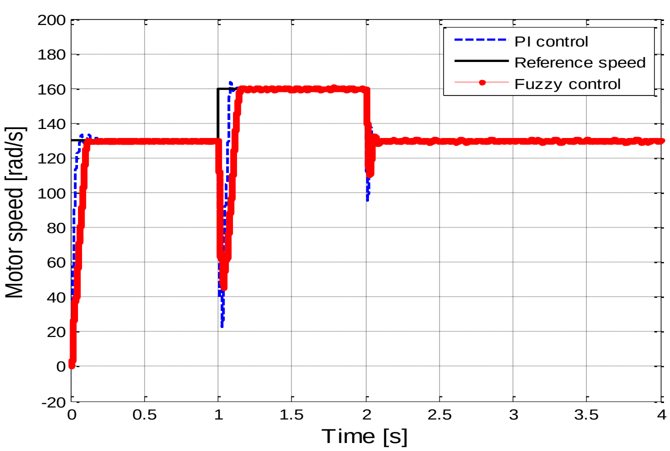

Fig.21: The motor speed variation response with PI and fuzzy controller with MPPT

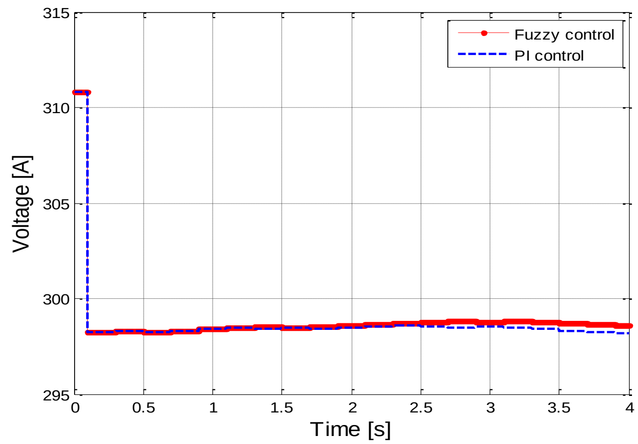

Fig. 22: The voltage of PV cell variation response with PI and fuzzy controller with MPPT

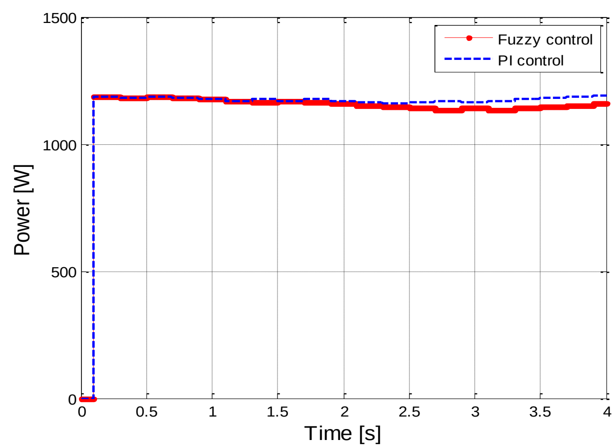

Fig. 23: The power of PV cell variation response with PI and fuzzy controller with MPPT

4.2. Speed Control without MPPT

Figure 24 shows the motor rms current variation response with PI and fuzzy controllers without using MPPT. The transitorily current peaks are higher than their corresponding values with using the MPPT technique illustrated in Fig. 20. Figure 25 depicts the motor speed variation response with PI and fuzzy controllers without using the MPPT. The voltage of PV cell variation response with PI and fuzzy controller without using the MPPT is illustrated in Fig. 26. Also, Fig. 27 shows the power of PV cell variation response with PI and fuzzy controller without using MPPT. In all last figures, it is shown that the induction motor speed and the motor rms current variation response are better with the proposed fuzzy logic controller than the conventional PI controller. In Fig. 27, the PV power transient behavior with a step speed rise at 1s is not good in both fuzzy logic and conventional PI controller without using MPPT.

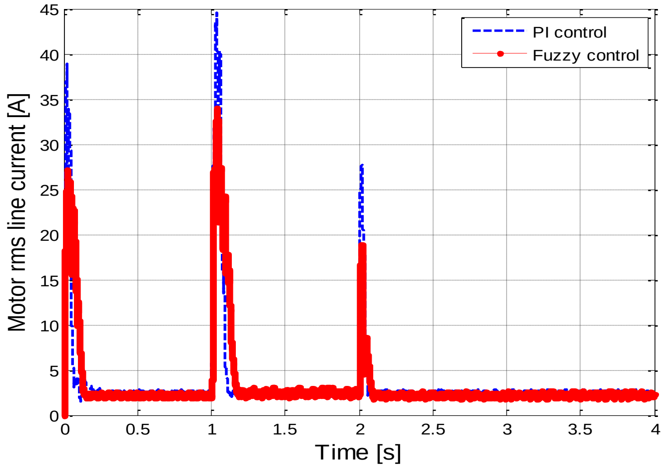

Fig. 24: The motor current variation response with PI and fuzzy controller without MPPT

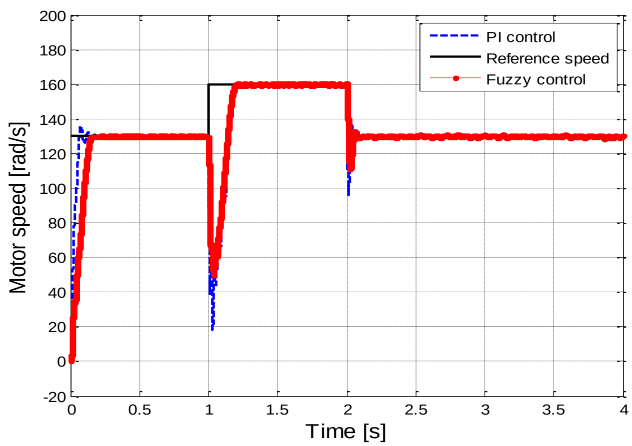

Fig. 25: The motor speed variation response with PI and fuzzy controller without MPPT

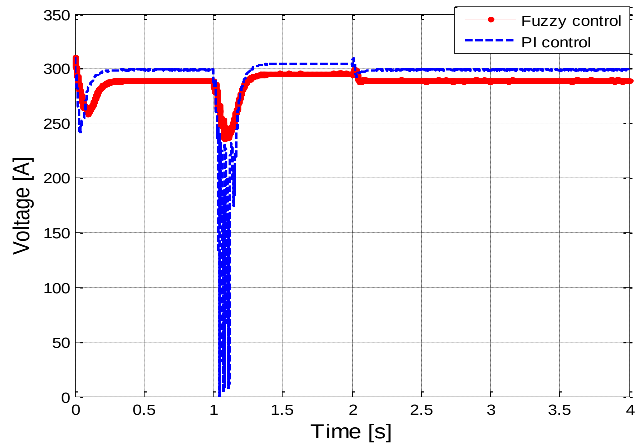

Fig. 26: The voltage of PV cell variation response with PI and fuzzy controller without MPPT

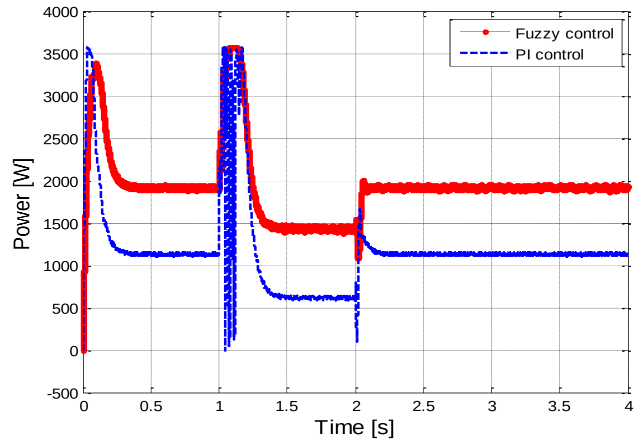

Fig. 27: The power of PV cell variation response with PI and fuzzy controller without MPPT

Figure 28 shows the voltage of PV cell variation response with and without MPPT in case of the proposed fuzzy control. The power of PV cell variation response with and without MPPT in case of proposed fuzzy control is shown in Fig. 29. The results illustrated in Figs. 28 and 29 show the superiority of the fuzzy logic controller in conjunction with the MPPT technique in enhancing the power and voltage performance of the PV array.

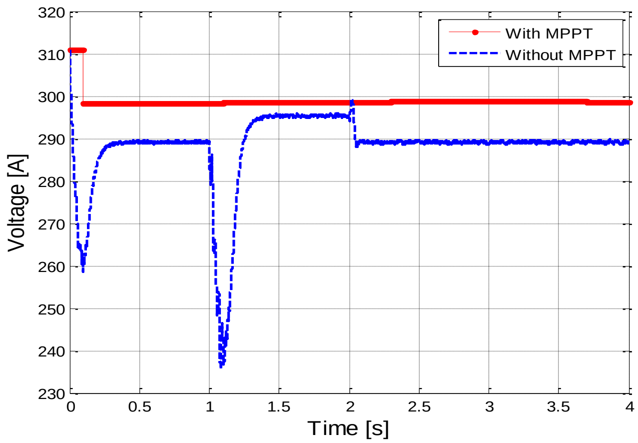

Fig. 28: The voltage of PV cell variation response with and without MPPT using fuzzy control technique

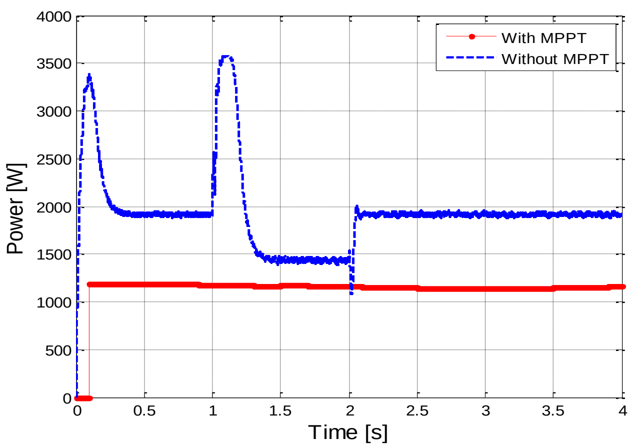

Fig. 29: The power of PV cell variation response with and without MPPT using fuzzy control technique

5. Conclusion

In this research, the fuzzy logic control design with space vector PWM for adjustable speed tracking applications is developed. With MPPT, the fuzzy and PI controllers are used to control the motor speed at variable speed and variable radiation with constant temperature for PV systems applications. Also, the conventional PI controller is designed and applied. Two three-phase inverter topologies are investigated. The V/F control technique is used to operate the SVPWM inverters. Compared to the universal bridge, the 2-level bridge inverter gives better speed performance with less distortion line to line voltage profile. In comparison to the conventional PI controller, the fuzzy logic controller accurately controls the speed of an induction motor. Furthermore, it significantly enhances the control system accuracy and the whole photovoltaic power system performance in both transient and steady state. This controller combines the advantages of the classical controller and the intelligent properties of the fuzzy logic controller. The results proved the superiority of the fuzzy logic control to track the motor speed variation.

6. Appendix A

The parameters of the three-phase induction motor used in simulations are given in Table A1 [15].

Table A1: Induction motor Parameters

Parameter	Value	Unit
Rated voltage	575	V
Number of poles	4	-
Rated power	5	hp
Rated frequency	60	Hz
Rated speed	1750	rpm
Stator resistance	2.053	Ω
Stator inductance	0.008	H
Rotor referred resistance	1.904	Ω
Magnetizing inductance	0.3144	H
Winding connection	star	
Moment of inertia	0.02	$Kg.m^2$
Friction coefficient	0.0025	N.m.s
Type	Squirrel cage	-

References

[1] J. Larminie, J. Lowry, "Electric Vehicle Technology Explained", John Wiley & Sons Ltd, 2nd ed., 2012.

[2] A. Gupta, L. Mathew, S. Chatterji, "V/f-based Speed Controller for an Induction Motor Using AI Techniques", Advances in Intelligent Systems and Computing, Springer India, Vol. 236, 2014, PP. 1161-1171.

[3] Ahmed M. Kassem, Ali M. Yousef, "Fuzzy-Logic Based Self-Tuning PI Controller for High-Performance Vector Controlled Induction Motor Fed by PV-Generator", Journal of Engineering

Science (JES), Assiut University, Vol. 40, 2012, PP. 1179-1193.
[4] S. Singh, P. Sharma, A. Varshney, Ankit Kumar, "Speed Control of Multilevel Inverter-Based Induction Motor Using V/F Method", Advances in Intelligent Systems and Computing, Springer India, Vol. 335, 2015, PP. 231-234.
[5] M. M. Gaballah, "Design and Implementation of Space Vector PWM Inverter Based on low Cost Microcontroller", Arab journal Sci Eng, Vol. 38, 2013, PP. 3059-3070.
[6] K. M. Rajani, R. P. Nikhil, "A Robust Self-Tuning Scheme for PI-and PD-type Fuzzy Controllers", IEEE Trans. On Fuzzy Systems, Vol. 7, 1999, PP. 2-16.
[7] K. M. Rajani, R. P. Nikhil, "A self-Tuning Fuzzy PI Controllers", Fuzzy Sets and Systems, Vol. 115, 2000, PP. 327-338.
[8] B. M. Mohan, A. Sinha, "Analytic Structure and Stability Analysis of a Fuzzy PID Controller", Applied Soft Computing, Vol. 8, 2008, PP. 749-758.
[9] W. Li, "Design of a Hybrid Fuzzy Logic Proportional Plus Conventional Integral-Derivative Controller", IEEE Trans. Fuzzy Syst., Vol. 6, 1998, PP. 449-462.
[10] Ali M. Yousef, A. S. Oshaba, "Efficient Fuzzy Logic Speed Control for Various Types of DC Motors Supplied by Photovoltaic System Under Maximum Power Point Tracking", Journal of Engineering Science (JES), Assiut University Vol. 40, 2012, PP. 1455-1474.
[11] M. Jabri, H. Chourif, H. Jerbi, N. B. Braiek, "Fuzzy Logic Parameter Estimation of an Electrical System", 5th International Multi-Conf on Systems, Signals and Devices, Amman, Jordan, June, 2008, PP. 1-6.
[12] A. El-Dessoky, "Adaptive Fuzzy Control for High Performance Induction Motor Drives", Royal Military College of Canada, Prorequest Dissertation, 2002.
[13] A. M. Kassem, Ali M. Yousef, “Robust MPPT Control Design and Dynamic Performance of a PV-Generator Powered DC-Motor Pump System”, 13th middle East Power System Conference IEEE, MEPCON’ 2009, Assiut university, Egypt, December 2009, pp. 379-384.
[14] B. K. Bose, “Modern Power Electronics and ac Drives”, New Jersey: Prentice-Hall PTR, 2011.
[15] A. Rubaai, M. Kankam, “Adaptive Tracking Controller for Induction Motor Drives Using Online Training of Neural Networks” IEEE Trans. Industrial Appl., Vol. 36, 2000, PP. 1285-1294.
[16] B. K Bose, "Power Electronics on ac Drives", Engewood Cliffs, New Jersey: Prentice-Hall, 1986.
[17] F. El-Sousy, M. M. Salem, "Robust neural Network Controllers for Indirect Field Orientation Control of Induction Machine Drive System ", Proc. of the International Conference on Control and Application, Xiamen, China, Vol. 1, 2002, PP. 1263-1268.
[18] Y. Yang, "Adaptive Perturb and Observe MPPT Technique for Grid Connected Photovoltaic Inverters", Procedia Engineering, Vol. 23, 2011, PP. 468-473.
[19] M. Srivastava, S. Agarval, E. Sharma, "Design and Simulation of Perturb and Observe MPPT Algorithm for 72 Cell Solar PV System", International Journal of Soft Computing & Engineering (IJSCE), Vol. 4, 2016, PP. 49-53.
[20] V. Kumaresh, M. Malhotra, N. Ramakrishna, R. P Saravana, K. Vijith, "A perturb and Observe Based Solar MPPT System for Stand-alone Applications", International Journal of Advancements in Electronics and Electrical Engineering (IJAEEE), Vol. 3, 2014, PP. 32-37.
[21] B. Bendib, F. Kri, H. Belmili, M. F., Almi, S. Bolouma, "An Intelligent MPPT Approach Based on Neural-Network Voltage Estimator and Fuzzy Controller, Applied to a Stand-alone OV System", IEEE 23rd Inter. Symposium on Industrial Elect. (ISIE), Istanbul, Turkey, Vol. 1, 2014, PP. 404-409.
[22] Krause, P.C., O. Wasynczuk, and S.D. Sudhoff, "Analysis of Electric Machinery" , IEEE Press, 2002.
[23] S. Panda, A. Mishra, B. Srinivas, "Control of Voltage Source Inverters using PWM/SVPWM for Adjustable Speed Drives Applications", B. Tech Thesis, 1133, National Institute of Technology, Rourkela, India, 2009.
[24] http://www.mathworks.com/matlabcentral/fileexchange/35911-svpwm-based-speed-control-of-induction-motor-with-3-level-inverter-using-vf-method/content/svpwm_IM.mdl